GEOPHYSICAL RESEARCH LETTERS, VOL. 24, NO.13, PAGES 1691-1694, JULY 1, 1997

The Brazil/Guará equatorial spread F campaign: Results of the large scale measurements

J. LaBelle and J.-M. Jahn
Department of Physics and Astronomy, Dartmouth College, Hanover, New Hampshire

R. F. Pfaff
Laboratory for Extraterrestrial Physics, NASA/Goddard Space Flight Center, Greenbelt, MD

W. E. Swartz
School of Electrical Engineering, Cornell University, Ithaca, New York

J. H. A. Sobral, M. A. Abdu, P. Muralikrishna, and E. R. dePaula
Instituto Nacional de Pesquisas Espaciais, São José dos Campos, Brazil

Abstract.
The Guará campaign equatorial spread F rocket was launched from Alcântara, Brazil, on 14 October 1994 at 1955 LT (2255 UT) into an active topside spread F event. Spread F plasma irregularities observed up to 822 km altitude correlate well with plumes observed simultaneously with a coherent backscatter radar. Matching 1–10 km features in the rocket and radar data over the altitude range 300–800 km implies an eastward drift speed of $\sim$ 110 m/s, versus 95 m/s at 400–500 km based on radar interferometry. Combining these two measurements implies an average upward drift of 30 m/s for the highest altitude structures. The amplitude difference between low- and high-altitude 10-km density structures, if attributed to temporal effects, implies an effective diffusion coefficient (decay time constant) of 500-1000 m^2/s ($2–4\times10^{-4}$ s^{-1}), which agrees with previous estimates from other techniques and supports the idea that the decay of spread F turbulence occurs in a scale-independent manner.

Introduction

Equatorial spread F (ESF) is a general term for processes that produce irregularities with spatial scales 10^{-2}–10^{6} m in the equatorial F-region. The primary energy source for the irregularities is gravity, but the microphysics of ESF on various scales and under various conditions is not well established, either experimentally or theoretically [review by *Kelley*, 1989]. Rocket experiments play a key role in ESF research by providing vertical cuts through the anisotropic irregularities and sensitivity to small scales. The 1994 Guará spread F rocket experiment was the first to measure ESF density and electric field irregularities at altitudes considerably above 600 km. The payload contained two antenna systems for measuring electric field and three independent electron density measurements: Langmuir probes, a Plasma Frequency Probe (PFP), and a capacitance probe. This paper focuses on large scale features (> 1 km) detected by this experiment, with emphasis on comparison of radar and rocket data.

Paper number 97GL00818.
0094-8534/97/97GL-00818$05.00

Data Presentation

The rocket was launched from Alcântara (2.4° S, 44.4° W) on October 14, 1994, at 1955 LT (2255 UT). It followed the planned trajectory ($\sim$ 36° east of due north, or $\sim$ 58° east of magnetic north) and achieved an apogee of 957 km at a range of 532 km, or 450 km east projected along the magnetic equator. Figure 1 shows geophysical conditions on the launch night. Figure 1*a* shows the relative amplitude of a 136.38-MHz beacon transmitted from GOES-1 and received at São Luis (2.6° S, 44.2° W), about 40 km from the rocket range. GOES-1 is situated west of the Alcântara/São Luis meridian, so that the beacon transmission path cuts through the F-region (at 400 km) approximately 300 km west of the rocket range. Strong amplitude scintillations set in at 2145 UT (1845 LT) and continue for several hours, including the entire rocket flight. The digital ionosonde at São Luis (Fig. 1*b*) shows that October 14 is characterized by a relatively intense pre-reversal enhancement electric field: the post-sunset rise in the virtual height of the F-layer ($h'F$) averages 20 m/s but reaches 40 m/s at times, and $h'F$ reaches 370 km at 2145 UT (1845 LT). Spread F starts at 2135 UT (1835 LT) and reaches its maximum range spreading, at 2300 UT (2000 LT), five minutes after launch. (Spread F index of 1, 2, or 3 implies range spreading < 100 km, 100–200 km, or > 200 km, respectively.) Figure 1*c* shows path-integrated total electron content (TEC) derived from the signal from a selected GPS satellite

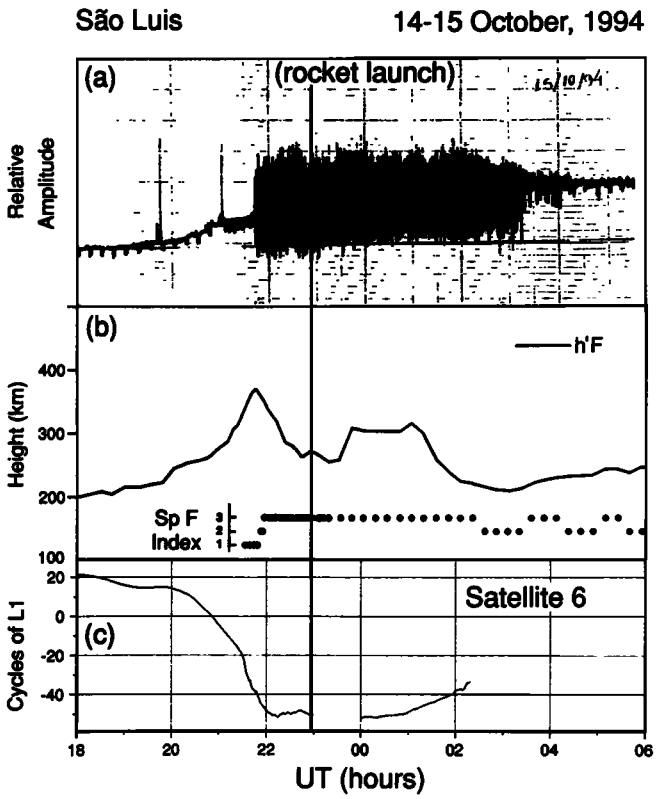

Figure 1. Geophysical conditions on October 14, 1994: (a) relative amplitude of a 136.38-MHz satellite beacon received at São Luis; (b) parameters measured with the digital ionosonde, including the virtual height of the F-peak ($h'F$) and the F-layer bottomside estimated two different ways ($h'F4$ and $hpF2$; see UAG Report 23 [1972]), as well as the spread F index; and (c) path-integrated TEC derived from the signal from a selected GPS satellite. Scintillations, spread F, and depletions in TEC set in shortly before the launch time, which is marked by an arrow.

which is over the rocket trajectory during the flight. The cosine variation of TEC with time results from geometric effects, but starting at 2140 UT (1840 LT) TEC fluctuations commence accompanied by a steep anomalous dropout in TEC, indicative of ESF related plasma depletions along the path.

The Cornell University Portable Radar Interferometer (CUPRI), described in a companion paper [*Pfaff et al.*, this issue], was used to determine the rocket launch time. Figure 2*a* shows the CUPRI RTI recorded between 1845 and 2000 LT on October 14, 1994. Backscatter from F-region irregularities starts shortly before 1850 LT, 4–5 minutes after the onset of VHF scintillations to the west (Fig. 1*a*). The radar echoes develop into multiple topside plumes extending to above 900 km. For almost the entire interval, the radar detects bottomside ESF irregularities which initially increase in altitude, reaching over 400 km near 1915 LT consistent with the ionosonde data, and which then descend to 220–260 km at 2000 LT. Two sets of topside structures appear: one complex set of plumes appears to break away from the bottomside spread F layer just before 1900 LT, while the F-region is still rising but near its highest point; a second set of plumes appears to break away from the bottomside layer near 1930 LT, as the F-region descends.

Because the radar measures the ionosphere directly overhead while the rocket collects data as far as 1000 km away, comparison of rocket and radar data requires mapping assumptions. Suppose that the irregularities are magnetic field-aligned, they do not evolve substantially during the half-hour drift time, and they drift eastward with a constant altitude-independent speed of 110 m/s; under these conditions, the portions of the radar RTI sampled by the rocket during the upleg would be those indicated by the solid line superposed on Figure 2*a*. (The 110 m/s drift speed provides the best fit

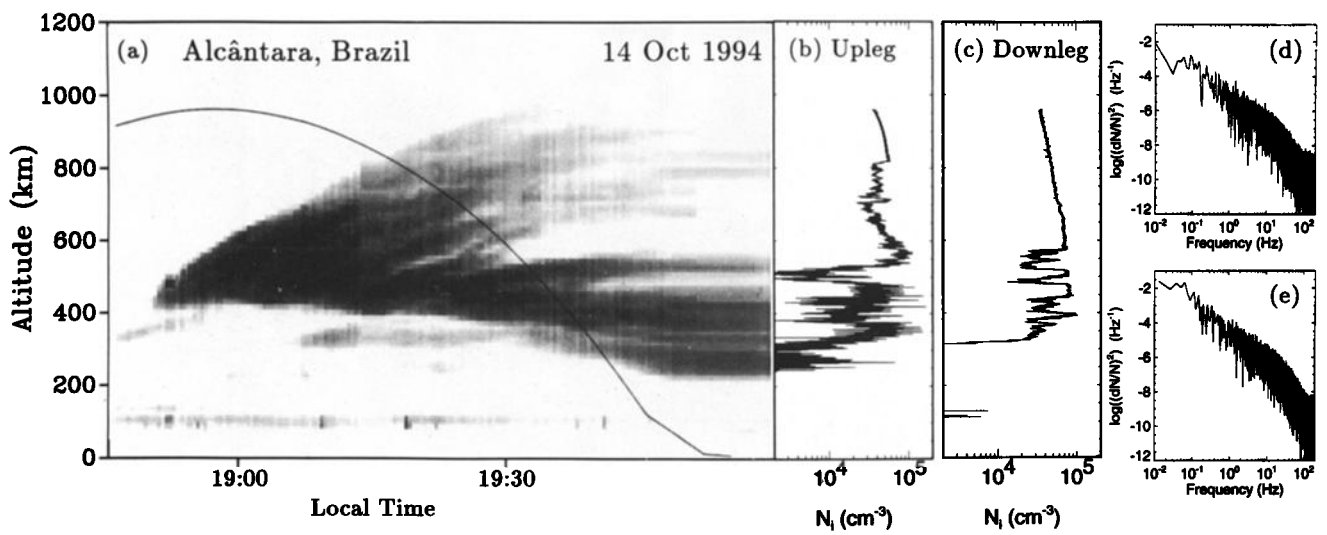

Figure 2. A comparison of radar and rocket data: (a) the CUPRI RTI for 1845–2000 LT on October 14; (b) the electron density profile measured with the Langmuir probe during the upleg portion of the rocket flight; (c) the correponding profile for the downleg; and spectra of density irregularities at (d) 600-800 km on the upleg and (e) 400-600 km on the downleg. The solid line in (a) shows an estimated rocket trajectory through the ESF structures detected by the radar.

between the radar and rocket data under these assumptions, although it is somewhat greater than the drift inferred from radar interferometry, as discussed below.) The rocket appears to fly "backward" in time; i.e., as the rocket moves eastward, it encounters regions which were overhead of Alcântara at earlier times.

For the upleg, Figure 2*b* shows the electron density inferred from the Langmuir probe current normalized to the PFP absolute density measurement at the F-peak. The rocket encounters the structured bottomside of the F-region starting at 250 km altitude and penetrates multiple plasma depletions up to 822 km. In some cases, electron density features are associated with features in the 3-m backscatter along the trajectory; for example, at about 500 km, the rocket encounters a deep density depletion ($< 10^{-4}$ cm^{-3}) at the same altitude where the estimated rocket trajectory intersects a plume of intense 3-m backscatter. Below 460 km on the upleg, the rocket data are contaminated by interference from the attitude control system (ACS), which appears as a series of regularly spaced spikes in the electron density.

During the downleg (Figure 2*c*), deep density depletions (70–80%) characterize the F-region at 315–570 km altitude. The gradients at the lower edges of these depletions are steeper than those at the upper edges, and the upper edges are more structured, providing evidence that the gravitational instability acts to limit the steepness of the unstable upward density gradients. This downleg profile looks similar to those measured in several previous rocket flights [e.g., *Kelley et al.*, 1982]. Most likely, these topside structures erupt from the bottomside layer to the east of Alcântara and are not detected with the radar.

Figures 2*d-e* show power spectra of density irregularities measured between 600–800 km on the upleg and 400–600 km on the downleg. The frequencies displayed, 0.01–200 Hz, would correspond to wavelengths in the range 10 m to 100 km if the turbulence were stationary on the time scale of the rocket's traversal through them. The spectra exhibit an $f^{-5/3}$ power law dependence At scales greater than $\sim$ 100 m and a break to a steeper power law at wavelengths shorter than about 100 m, as reported from previous rocket flights [e.g., *Kelley et al.*, 1982]. The low altitude spectrum contains more power, but the two spectra have similar spectral shapes at wavelengths greater than 1 km.

In order to facilitate comparison of the rocket and radar data, Figure 3*a* (top panel) shows the intensity of the fluctuations in the electron density detected by the rocket, integrated over the frequency range 50–250 Hz, as a function of altitude. Figure 3*b* shows the intensity of the 3-m backscatter along the hypothetical rocket trajectory shown in Figure 2*a*. Figure 3*c* shows electron density fluctuations ($\delta n/n$), filtered to remove the low frequency variations, and Figure 3*d* (bottom panel) shows the unfiltered electron density. At altitudes above 460 km, broad maxima in the integrated power of the rocket-measured density flucutuations at 490–535 km, 640–740 km, and 780–820 km are roughly correlated with maxima in the CUPRI backscatter power along the hypothetical trajectory. The relatively short burst of density irregularities observed with the rocket but not with the radar at 580–600 km presents an exception,

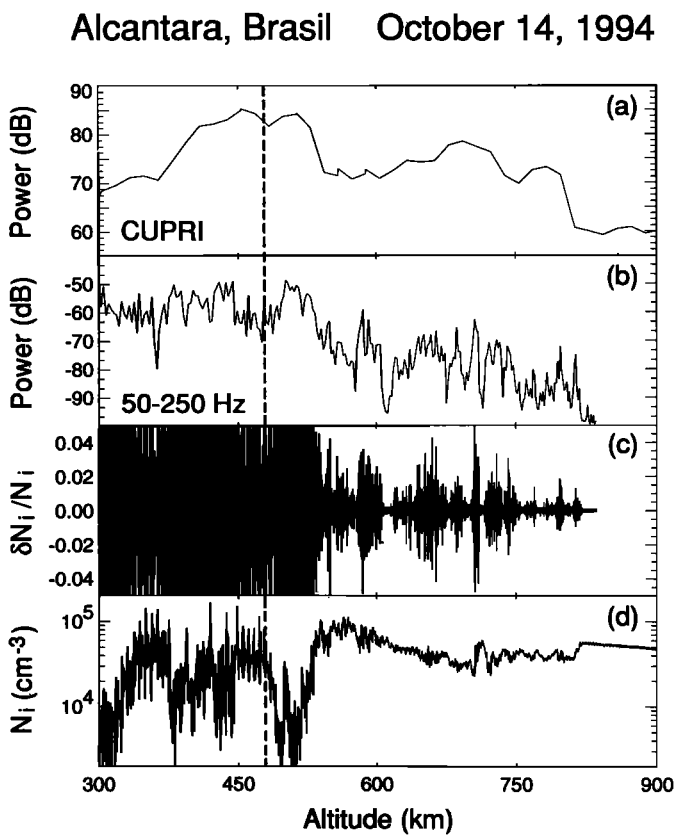

Figure 3. (a) intensity of electron density fluctuations detected by the rocket, integrated over 50–250 Hz; (b) intensity of 3-m backscatter along the hypothetical rocket trajectory shown in Figure 2*a*; (c) electron density flucuations, filtered to remove low frequencies; and (d) the unfiltered electron density. Above 460 km, broad maxima in the integrated power of the rocket-measured density flucutuations are roughly correlated with maxima in 3-m backscatter power. Rocket data below 460 km are contaminated by payload system interference.

but such short scale features may be subject to greater time variability than the broad enhancements. Below 460 km, the integrated power of the rocket-measured density fluctuations cannot be compared with the radar backscatter power due to the ACS interference.

Discussion

The good match between radar and rocket features at several altitudes indicates that the mapping assumptions used in comparing the data have some validity. In particular, the drift speed of 110 m/s inferred from optimizing the match between the rocket and radar data may be interpreted as an approximate speed of the drifting topside structures, averaged over $\sim$ 30 minutes and 300-800 km. The radar interferometer provides an independent measurement of the drift, if the 3-m irregularities may be considered tracers of the larger structures. Some of the interferometer data are ambiguous due to unexpectedly large Doppler shifts; however, in the altitude range 400–500 km at approximately 1925 LT, the interferometer data imply drifts the order of 95 m/s, about 20% lower than the estimate from the

rocket-radar comparison. The difference may be due to the different time and altitude averaging inherent in these measurements. Alternatively, the rocket-radar comparison may overestimate the drift because it does not account for the ascent of the large scale features during the ~ 30-minute delay between the radar and rocket measurements. Taking 95 m/s to be the actual drift, the altitude at which the rocket leaves the turbulent regions (822 km) exceeds the altitude predicted from the radar data (740 km); the difference can be accounted for by a vertical rise velocity of 30 m/s for the rising ESF bubble over that altitude range, corresponding to a zonal electric field of 0.5 mV/m. This bubble rise velocity is a factor 2–3 smaller than typically observed in previous experiments, for example San Marco-D [*Aggson et al.*, 1992], and predicted theoretically [e.g., *Ott*, 1978]; however, there is much case-to-case variation, and there is evidence that the bubble rise velocity decreases at high altitudes [e.g., *Dabas and Reddy*, 1990].

The rocket electron density profiles reveal significant differences between density structures encountered on the upleg within the high-altitude radar plume, on the upleg within the low-altitude radar plume, and on the downleg where there are no corresponding radar measurements. The downleg structures are relatively deep and sharply defined, with turbulence restricted to the gravitationally unstable upper boundaries of the depletions. The low-altitude upleg density depletions are also relatively deep. But the high-altitude upleg structures consist of less deep density depletions (< 50%), and density fluctuations at high altitudes on the upleg are not concentrated on the gravitationally unstable gradients but are distributed over a broad altitude range. Except for the power level, the spectra of density irregularities associated with these regions exhibit similar $f^{-5/3}$ power laws.

One interpretation of these differences is that they result from temporal evolution. Since the assumptions used to map the rocket trajectory onto the radar RTI are supported by the good correlation between the rocket and radar data, one may be justified in using the radar data to to place limits on the age of features encountered by the rocket. The high-altitude plume on the upleg erupts from the bottomside at about 1900 LT and is thus at least 70 minutes old when the rocket flies through it. The low-altitude plume separates from the bottomside at 1930 LT and is thus at least 35 minutes old when encountered by the rocket. The downleg density depletions may be younger still since CUPRI did not detect them. The 10-km scale depletions in the low altitude structure are much deeper than those in the high altitude structure. This observation agrees qualitatively with previous radar and scintillation experiments which show that km-scale structure persists after backscatter radar echoes disappear [*Basu et al.*, 1978]. Assuming that the field-aligned structures are subject to dissipation via diffusion ($k_\perp^2 D$, where $k_\perp$ is the wavenumber perpendicular to the magnetic field), and interpreting 40–80 minutes as the e-folding time for 10-km structures, one infers an effective diffusion coefficient (decay time constant) of 500-1000 m^2/s ($2–4\times10^{-4}$ s). This estimated effective diffusion coefficient (decay time) should be considered an upper (lower) bound, since the topside eruptions may have originated earlier than their appearance in the CUPRI RTI, but certainly not later. The smaller number (500 m^2/s) is consistent with previous estimates of the diffusion coefficient associated with Barium cloud striations [*Lebeda et al.*, 1984] and with intermediate scales in ESF [*LaBelle et al.*, 1986]. Interestingly, the decay time constant of 2×10^{-4} s is identical to that inferred by *Hysell* [1992] from measuring the decay of ESF structures encountered on successive AE-E satellite passes. As in the AE-E data, the Guar'a rocket-measured spectra retain the $f^{5/3}$ power law as they decay, which supports the idea that the decay of ESF irregularities is characterized by a single decay time constant at all scales (M.C. Kelley, personal communication, 1996).

Acknowledgments. The authors acknowledge excellent engineering support by the NASA team led by Mr. David Kotsifakis. The authors thank the Brazilian Air Force and the Brazilian Space Agency (INPE) for range support. This research is supported by NASA grants NAG5-663 and NAGW-5071 to Dartmouth College and NAG5-666 to Cornell University.

References

Aggson, T.L., et al., Equatorial bubbles updrafting at supersonic speeds, *J. Geophys. Res., 97*, 8581, 1992.

Basu, S., et al., On the coexistence of kiliometer- and meter-scale irregularities in the nighttime equatorial F-region, *J. Geophys. Res., 83*, 4219, 1978.

Dabas, R.S., and B.M. Reddy, Equatorial plasma bubble rise velocities determined from multistation scintillation observations, *Radio Sci., 25*, 125, 1990.

Hysell, D.L., *On the Hierarchy of Processes Contributing to Equatorial Spread F*, PhD thesis, Cornell University, p. 217, 1992.

Kelley, M.C., *The Earth's Ionosphere*, Academic Press, San Diego, 1989.

Kelley, M.C., et al., Simultaneous rocket probe and radar measurements of ESF: transitional and short wavelength results, *J. Geophys. Res., 87*, 1575, 1982.

LaBelle, J., M. Kelley, and C. Seyler, The role of drift waves in spread F, *J. Geophys. Res., 91*, 5513, 1986.

Lebeda, C., S.P. Gary, and M. Pongratz, Density spectra as a function of altitude in an ionospheric Barium release, *Geophys. Res. Lett., 11*, 591, 1984.

Ott, E., Theory of Rayleigh-Taylor bubbles in the equatorial ionosphere, *J. Geophys. Res., 83*, 2066, 1978.

UAG Report 23, *URSI handbook of ionogram interpretation and reduction*, World Data Center A, U.S. Dept. of Commerce, NOAA, Boulder, Colorado, 1972.

Zargham, S., and C.E. Seyler, Collisional interchange instability, 1, Numerical simulations of intermediate scale irregularities, *J. Geophys. Res., 92*, 10073, 1987.

J. LaBelle and J. M. Jahn, Department of Physics and Astronomy, Dartmouth College, Hanover, NH 03755

R. F. Pfaff, Laboratory for Extraterrestrial Physics, Goddard Space Flight Center, Greenbelt, MD 20771

W. E. Swartz, School of Electrical Engineering, Cornell University, Ithaca, NY 14853

M. A. Abdu, E. R. dePaula, P. Muralikrishna, and J. H. A. Sobral, Instituto Nacional de Pesquisas Espaciais, Av. de los Astronautas 1758, São José dos Campos, Brazil

(Received August 26, 1996; revised January 28, 1997; accepted February 28, 1997.)